EXPERIMENTAL STUDY OF SHOCK WAVE DYNAMICS IN MAGNETIZED PLASMAS

DOE AWARD NO. DE-FG02-04ER54792

AD - FINAL REPORT

REPORTING PERIOD: 2004 -2008

OFFICE OF SPONSORED PROGRAMS, TROY STATE UNIVERSITY, TROY, AL

PROJECT DIRECTOR: DR. NIRMOL PODDER

PHONE: 334-670-3409, FAX: 334-670-3587

Abstract

In this four-year project (including one-year extension), the project director and his research team built a shock-wave–plasma apparatus to study shock wave dynamics in glow discharge plasmas in nitrogen and argon at medium pressure (1–20 Torr), carried out various plasma and shock diagnostics and measurements that lead to significant progress in understanding shock wave acceleration phenomena in plasmas. Specifically, the team has

- completed the construction of spark-discharge shock tube in the first year;
- optimized the shock tube over low Mack numbers (Mach 1–4);
- built a microwave target plasma and optimized the steady-state plasma condition;
- carried out various probe and spectroscopic diagnostics for the dc glow plasma;
- launched acoustic shock waves in three different plasma conditions: (i) steady-state, (ii) pulsed or transient, (iii) afterglow plasma;
- studied turbulence and the shock wave behaviors in the glow discharge plasmas;
- performed a comprehensive set of measurements and computations to increase our understanding of shock-plasma correlation behaviors and improve our understanding of shock acceleration mechanisms in discharge plasmas.

The measurements clearly show that in the steady-state dc glow discharge plasma, at fixed gas pressure the shock wave velocity increases, its amplitude decreases, and the shock wave disperses non-linearly as a function of the plasma current. In the pulsed discharge plasma, at fixed gas pressure the shock wave dispersion width and velocity increase as a function of the delay between the switch-on of the plasma and shock-launch. In the afterglow plasma, at fixed gas pressure the shock wave dispersion width and velocity decrease as a function of the delay between the plasma switch-off and shock-launch. These changes are found to be opposite and reversing towards the room temperature value which is the initial condition for plasma ignition case. The observed shock wave properties in both igniting and afterglow plasmas correlate well with the inferred temperature changes in the two plasmas.

I. Introduction

The PI and his team have made significant progress toward understanding shock wave acceleration, attenuation, and dispersion in low pressure non-thermal, non-equilibrium plasmas ($T_e >> T_i$). The construction of the shock tube with a built-in non-thermal glow discharge plasma and the associated probe diagnostics were completed in the first year of the proposal. The setup of the shock wave production mechanism along with the photo acoustic laser deflection technique and pressure sensor diagnostic for the shock wave was completed in the second year. Most of the third year was devoted to the shock wave propagation measurements in the steady-state glow discharge plasma, and the fourth year to the pulsed discharge and afterglow plasmas.

In the first phase of the experiments, acoustic shock waves were launched in steady-state glow discharge plasmas, and shock wave properties were measured with photo acoustic laser deflection technique, pressure sensors, and high speed video cameras. All three measurements have revealed that an increase in the shock wave velocity results compared to the unionized case together with a decrease in the shock wave strength and the broadening (dispersion) of the shock-front. These modifications of shock waves in plasma have been attributed mainly to two different causes. A group of researchers argued that the plasma-specific effect is the main cause of shock wave acceleration and dispersion.[1-3] It is reasoned that the formation of double-layer electric sheaths at the propagating shock-front and the associated recirculation current and potential jump connected with the shock wave result in local neutral gas heating causing the shock dispersion and the shock-speed increase.[1-3] Another group of researches showed by combined experiments and simulations that the thermal non-uniformity and temperature variation in the discharge tube have been the primary cause of the shock wave modification in plasmas.[4-8] They have isolated the thermal effects from all other mechanisms in the plasma by pulsing the discharge on a short time interval.

In a steady-state glow discharge plasma column, temperature gradients are always present. Radially, the gas temperature assumes maximum at the tube-center but falls off nonlinearly towards the wall which stays very close to the room temperature. In addition, there are longitudinal variations of the temperature starting from the anode to cathode. Various regions of the anode and cathode glow regions assume different temperatures. Thus, it has been nearly impossible to completely isolate the plasma-specific effects from the thermal mechanisms in the steady-state dc discharge plasma. The net plasma effects plus the gas temperature variations and non-uniformities cause apparent broadening and splitting in the shock wave profile. However, a pulsed plasma has been used to isolate the thermal mechanisms from the plasma-specific effects, and the result of which indicate that the shock wave dispersion and acceleration are primarily associated with the increase in the discharge gas temperature.

II. Experimental Apparatus and Diagnostics

A spark-discharge shock tube along with the built-in plasma section is established in the Laboratory for the shock wave dynamics experiments (see Fig. 1). The entire shock tube is 1.6 m long and comprised of a series of small Pyrex glass cylinders, each 38 cm long and 3.5 cm in inner diameter. Each of these small Pyrex tubes has a stainless steel Conflat flange on both sides, which provides easy attachment with one another to make up the entire shock tube assembly.

The key components of the shock tube apparatus are: (i) the vacuum pump and gas flow control systems, (ii) the test section (plasma or afterglow) plus neutral gas sections, and (iii) the spark-gap section. Some of the key diagnostics used in the experiment are electrical and high voltage probes for plasma parameters, lasers and pressure sensors for shock wave properties.

Fig 1: Photograph of the shock tube and the associated diagnostics. The molecular nitrogen plasma (bright orange glow) is shown in the 38-cm long discharge section. Laser beam deflection and high speed camera diagnostics can be seen. Shock waves are launched from above as indicated by the arrow.

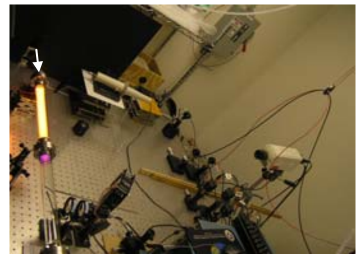

The vacuum pump system of the shock tube is comprised of a dry pump and a tubbomolecular pump. The dry pump (speed 3.7-liter/s and nominal pressure ~ 50 mTorr) and the turbomolecular pump (top speed 220 liter/s) work together to bring the system to a good vacuum at the base pressure ~ 10^{-5} Torr in about 30 min. At this point, the turbo pump is tuned off but the dry pump is kept running continuously. The gas cylinder line and the mass flow controller gate are opened to ultra-high purity (99.99%) argon or nitrogen gas. By setting the flow meter reading between 5–50 sccm, a continuous flow of argon is maintained to achieve the desired fixed pressure level. This volume flow rate creates a negligible motion (maximum speed 0.1 cm/s) of the gas medium inside the tube through which the shock wave is launched. The internal gas pressure is monitored by two absolute pressure Baratron gauges (0–100 Torr with a reading accuracy of 0.25% of the full-scale, and 0–1 Torr with a reading accuracy of 0.12%).

The plasma section of the shock tube is situated approximately in the middle of the shock tube and inside a single 38-cm Pyrex tube. The cylindrical hollow Conflat flanges on both sides of the Pyrex tube is used as electrodes for the glow discharge plasma. Typical experimental operating conditions are gas pressure from 1–30 Torr, glow discharge current 0–150 mA, break-down voltage 1–5 kV. The plasma is switched on by a 5.0 kW (0–5 kV, 0–1.0 A) dc power supply, either manually for the steady-state plasma condition, or remotely by a 6-V square pulse from the delay generator for the pulsed plasma and afterglows. The pulsed plasma is switched on for a period of less than one second at a time. In each run a shock wave is launched starting with a large delay between the plasma switch-on and the shock-launch. In the subsequent runs this delay is decremented in equal time intervals up to the plasma switch-on time. A similar series of measurements are also preformed starting at the extinguishing-point of the discharge. Thus, complete time histories of the shock wave modifications by the igniting and afterglow plasmas are produced.

Shock waves are launched from a spark-gap (electrode spacing 7.9 mm) connected to a high voltage capacitor (measured capacitance 2.8 μF, 0–15 kV dc) with charging voltage 8–18 kV. At a given capacitor charging voltage of 12 kV, the stored electrical energy is about 202 J, which is capable of producing a supersonic (~ Mach 2) acoustic shock wave in neutral argon at the room temperature (300 K). The spark-gap section of the shock tube is gradually curved into vertically downward direction to prevent any UV radiation originating from the spark to pre-ionize the gas volume in front of the propagating shock wave (sketch shown in Fig. 2). This configuration also prevents visible radiation from saturating the photo detectors. Moreover, the entire spark-gap plus capacitor system are placed inside a light-tight housing.[9,10]

Fig 2: Sketch of the shock tube and the associated diagnostics. Each laser beam crosses the plasma tube perpendicularly, and is sensitive to the density gradients associated with the shock-front.

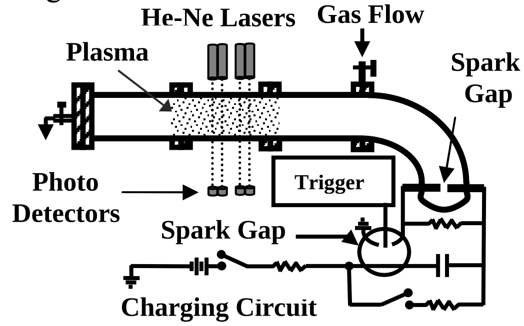

Steady-state plasma and electric-field characteristics are diagnosed with various electrical and high voltage probes. A sample measurement of plasma parameters using single Langmuir and floating double probes at a fixed current of 35 mA (and corresponding current density J = 3.6 mA/cm^2) in the range of gas pressures from 3–18 Torr yields an electron number density ~ 10^9 cm^{-3} and electron temperature ~ 1 eV at fixed pressure of 0.5 Torr and in the range of discharge currents I = 0–150 mA.[9,10] A pair of high voltage probes (Tektronix Model P6015A, bandwidth 75 MHz) is used to measure the floating potentials. From the two-point measurement of the floating potentials (two high voltage probes were separated by 2.6 cm), an average electric field strength of E = 6.3 V/cm is determined in the argon positive column plasma at a fixed pressure of 0.25 Torr and in the range of discharge currents 0–50 mA. This data yields an estimated reduced electric field strength (E/n_o) ~ 7×10^{-16} V·cm^2 or 70 Td at the room temperature of 300 K, where 1 Townsend (Td) = 10^{-17} V.cm^2.

Shock wave profiles in the plasma are measured with the photo acoustic deflection (PAD) technique of laser beams. Four pairs of laser beams (10-mW He-Ne laser, λ = 632.8 nm) are set up in the positive column plasma through the center of the tube. Each laser beam crosses the tube perpendicularly before it is received by a photo detector. All detector positions are adjusted to read half of the maximum intensity of the lasers. Thus, when a shock wave travels past the laser beams, it deflects them toward the maximum intensity due to the changes in the refractive index (proportional to the gradient in the shock-front gas density), and causes a positive jump in the photo detector's voltage. These voltage jumps are then recorded on the oscilloscope. Shock waves are either launched from the anode-side of the glow discharge that avoids encounter with the cathode regions and the hot electrons there, or alternately from the cathode side of the discharge. In each propagation polarity, shock waves move in the direction parallel to the glow discharge electric field direction, or anti-parallel to the electric field.

III. Experimental Results

A. Steady-State Glow Discharge Measurements

A steady-state plasma condition is achieved by keeping the plasma on for 15 min or longer before a shock wave is launched. Two 20-mW He-Ne laser beams (each was split into four beams using beam splitters and mirrors) are used to carry out eight-point measurements along the shock tube. The laser beams are sensitive to the refractive index modulation caused by the gradient in the shock wave gas density and deflected at the onset of the shock wave propagation. These deflections of the laser beams are recorded as voltage spikes in the photo detectors connected to the oscilloscopes, which give the arrival times of the shock wave and the structure of the shock-front. A typical example of the photo-acoustic deflections (PAD) by the shock wave in the case of neutral gas and the steady-state glow discharge plasma in Ar at fixed pressure P = 3.6 Torr and charging voltage V_{cap}= 12 kV, is shown in Fig. 3.

Fig 3: (a) Photo-acoustic deflection (PAD) signals obtain for neutral Ar gas at I = 0 mA, and (b) for plasma at fixed discharge current I = 70 mA. The noted differences between these pairs of signals are: (i) the shock wave took less time in plasma than in neutral gas, (ii) PAD signal strength is reduced in plasma, and (iii) shock wave profile is broadened or dispersed.

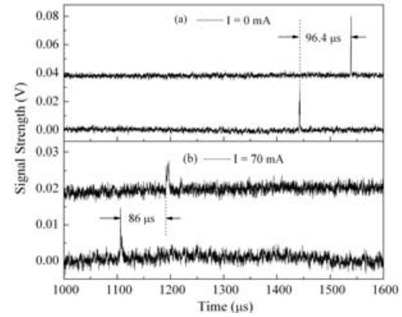

For the shock wave propagation in the neutral argon (I = 0 mA), the time difference between the first pair of PAD signals in Fig. 3(a) is 96.4 μs, and their spatial separation is 5.15 cm. This data yields a speed of 534.2 m/s for the shock wave in the neutral gas. In the same manner, the time difference between the second pair in Fig. 3(b) is 86 μs, and their spatial separation is 5.20 cm, which yields a speed of 598.8 m/s in the plasma at fixed glow discharge current I = 70 mA. These results and the deflection profiles in Fig. 3(b) indicate that a shock wave is accelerated, attenuated, and dispersed while traveling in plasma.[9,10]

Clear indications of shock wave dispersion as a function of the glow discharge current are shown in Fig. 4: (a) for gas pressure P = 3.6 Torr and (b) for P = 15 Torr at capacitor charging voltage V_{cap}= 12 kV. These measurements are performed long after the discharge was switched-on, or at the steady-state discharge condition. The laser deflection signals at both pressures show attenuation and an increasing widening of the shock-front as the plasma current is increased.[9]

Fig 4: Laser deflection profile at incremental plasma currents: (a) for argon discharge at 3.6 Torr, (b) at 15 Torr. Noted key features are (i) increased attenuation and (ii) increased widening (dispersion) and splitting as the current is increased. The splitting of the deflection profile is more pronounced at higher pressures.

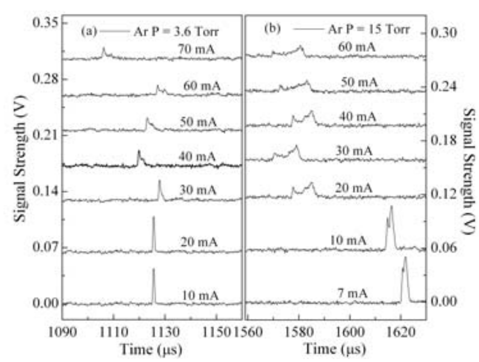

Shock wave dynamics are also captured on a high-speed camera that was obtained from Princeton Plasma Physics Laboratory (PPPL) last summer as part of an outreach program to aid in the collaborative research efforts. The high-speed Phantom 4 CMOS camera recorded the events in the glow discharge Ar and N_2 plasmas at a frame rate in access of 43,000 fps. The camera was set to take photographs of the shock wave every 23 μs interval (with 10 μs exposure time) as it travels through the plasma for various operating conditions. Five sample frames for the Ar and N_2 plasmas at about 70 μs interval are shown in Fig. 5. As the shock wave enters the Ar plasma, the shock wave suppresses the emissions from the atomic transition states, which is indicated by the dotted line in Fig. 5(a) right after the dark region. On the other hand, when the shock wave propagates in the molecular N_2 plasma, the emissions from the shock-front are enhanced as indicated by the dotted line in Fig. 5(b). The frame-by-frame analysis of the videos

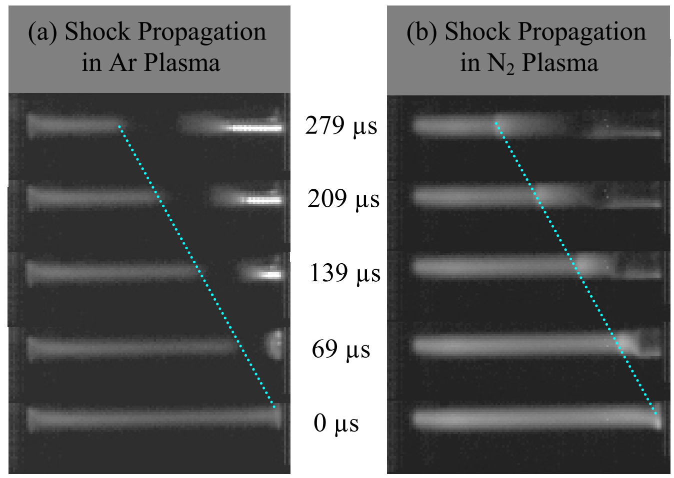

Fig 5: High-speed camera images for (a) argon plasma at fixed P = 15 Torr, I = 60 mA, and (b) N_2 plasma at P = 2 Torr, I = 50 mA. For both cases, the capacitor charging voltage V_{cap} = 12 kV, time is set to zero when the shock wave arrives at the plasma electrode. Ar plasma is quenched but the nitrogen molecular emissions are enhanced at the shock- front.

permits velocity measurements for the shock waves. Average shock wave velocities obtained from the high speed photography and the laser deflection technique are shown in Fig. 6 for the nitrogen plasma. The propagation velocity increases linearly with increasing discharge currents at fixed pressure. There is a good agreement between the video and laser measurements.[11]

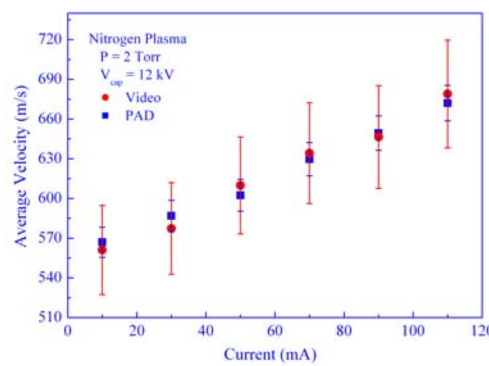

Fig 6: Comparison of velocities from the videos and the laser deflections for the nitrogen plasma at fixed pressure 2 Torr and capacitor charging voltage 12 kV. The measurement errors are about 6% for the video analyses and 2% for the laser deflection data.

B. Pulsed Plasma Measurements

In order to investigate the time-dependant effects on the propagating shock wave, a pulsed glow discharge plasma was produced for the duration of less than one second at a time.[12] On each run a shock wave was launched into the plasma in order to keep track of the plasma switch-on time (t_{on}) so that the delay time for the shock-launch ($\Delta t = t_s - t_{on}$) with respect to t_{on} can be determined. The time evolution of the shock wave profile at various fixed delays is shown in Fig. 7(a). For the purpose of easy identification, the corresponding delay time ($\Delta t = t_s - t_{on}$) of the shock wave with respect to the plasma switch-on time (t_{on}) are labeled on each laser deflection (PAD) profile. The horizontal coordinate in Fig. 7(a) represents a relative time which has been shifted in order to make room for each deflection profile on a uniformly-spaced graph. When the delay is near zero (Δt = 0.01 ms), the laser deflection signal yields a sharp delta-function-like profile. As the delay Δt increases, the PAD profile of the shock wave starts to dampen and broaden. At Δt = 30.20 ms, the PAD profile apparently splits into two peaks while the overall shape of the signal still keeps widening. At a delay of about 120 ms, the maximum attenuation and broadening of the PAD profiles have been reached in the plasma since no further change is visible in the subsequent runs. A relatively fixed laser deflection profile after a delay of about Δt

= 120 ms indicates that the plasma has already reached a saturation point (or steady-state condition).

In order to investigate the velocity changes as a function of delay, an average velocity of the propagating shock wave is determined at the fixed mid-point of the first pair of lasers which is 89 cm away from the spark gap. As an example, the typical time evolution of the average shock wave velocities for fixed discharge current I = 35 mA and gas pressure P = 15 Torr is shown in Fig. 7(b). Near the plasma switch-on time ($\Delta t = 0.0$ ms), the gas medium inside the tube is still at the room temperature (300 K), where the shock wave propagation velocity is measured to be about 530 m/s. As the delay is increased, the average shock velocity increases rapidly and nonlinearly. The average propagation velocity saturates to about 570 m/s at a delay of about 120 ms, after which no more changes in the velocities is visible. The measured trend in the shock wave velocity indicates that the plasma has reached a steady-state condition at a higher discharge gas temperature compared to its initial room temperature (~300 K). Next, the widths of the laser deflection (PAD) profiles are also analyzed as a function of the delay ($\Delta t = t_s - t_{on}$). Here, the changes in width data have been consistent with those in the average velocity data as shown in Fig. 7(b). Both the velocity and width data indicate that the igniting plasma quickly reaches a stead-state condition at a higher temperature ($T_g > 300$ K) after a delay ~ 100 ms, which is consistent with the earlier measurements by Macheret *et al*.[5] A similar trend has also been observed at other fixed pressures and plasma currents.

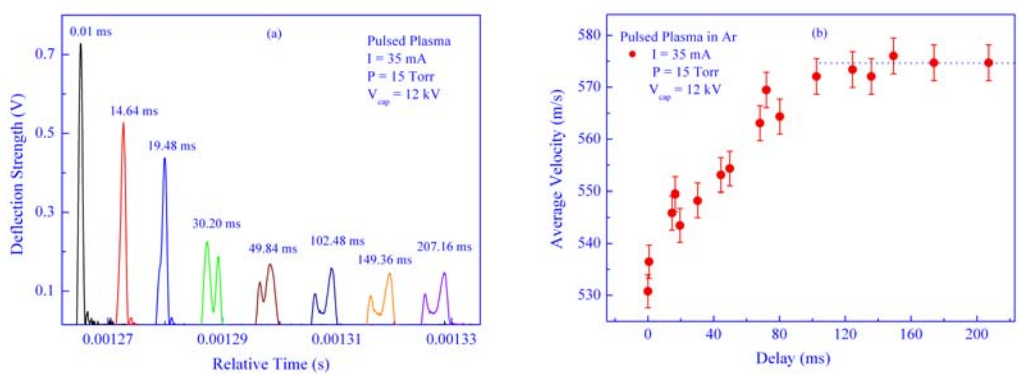

Fig 7: (a) Evolution of the shock wave profiles at fixed delays (delay time is shown on top of each PAD profile) in reference to the time ($t_{on} = 0$ ms) at which the plasma is switched on, (b) corresponding changes in the velocity of the shock wave. Shock wave velocity saturates in the plasma about 120 ms after its switch-on.

C. Afterglow Plasma Measurements

A similar study was also performed at the afterglow of the plasma or at the switch-off.[12] The time evolution of the shock wave profile in the afterglow plasma at various delays is shown in Fig. 8(a). A series of shock waves were launched starting with a shock wave launch-time t_s = 1000 ms (at the extinguishing point of the plasma), and incrementing it by 5 ms in consecutive runs. In this way the delay time ($\Delta t = t_s - t_{off}$) for the shock-launch is determined with respect to the plasma switch-off time (t_{off}). On Fig. 8(a), the delay time corresponding to each profile is labeled in reference to the plasma switch-off time, where the horizontal coordinate represents a relative time which has been shifted in order to make room for each deflection profile on a uniformly-spaced graph. At the plasma switch-off time (Δt = 0 ms), the laser deflection profile is still apparently split, attenuated, and broadened. As the delay is increased, the PAD profile starts to rise and narrow down while the apparent split structure becomes less and less distinct. At around a delay of 56 ms, the laser deflection profile attains its original delta-function-like single peak structure that was typical of the shock wave profile in the room temperature gas. Hence, the laser deflection profile in the afterglow plasma completely reverses to the original room temperature state which was first observed at the plasma switch-on (see the profile at Δt = 0.01 ms in Fig. 7(a)).

Typical changes in velocities in the afterglow plasma as a function of the delay time ($\Delta t = t_s - t_{off}$) is shown in Fig. 8(b) for fixed discharge current I = 35 mA and gas pressure P = 15 Torr. The average velocity is determined every time at a fixed location (the mid-point of the first pair of lasers which is 89 cm away from the spark gap) of the plasma tube. Near the plasma switch-off time (delay Δt = 0.0 ms), the shock wave propagation velocity is measured to be 570 m/s when the plasma is at its steady-state condition at T_g > 300 K. As the delay is increased, the average propagation velocity starts to drop. Here, the velocity changes take place roughly linearly in the afterglow plasma. After a delay of about 60 ms, the average propagation velocity of the shock wave reaches its initial room temperature value of about 530 m/s after which no more changes is noticeable. This is the value that was measured at the plasma switch-on (see Fig. 7(b)), thus confirming the reversing trend of the velocity, which one would expect in the afterglow plasma. The widths of the laser deflection (PAD) profiles in the afterglow plasma are also analyzed as a function of the delay ($\Delta t = t_s - t_{on}$). As a function of the delay time, a nonlinear behavior of the width similar to the velocity data in Fig. 8(b) is observed. It is also observed that the highly attenuated and apparent split profile at the steady-state plasma condition returns to its narrow, delta-function-like structure at this time. A similar trend has also been observed at other fixed pressures and discharge currents.

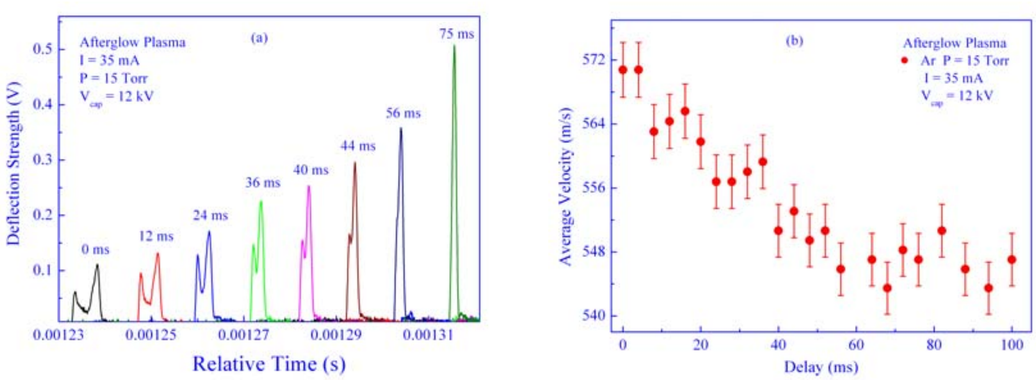

Fig 8: (a) Recovery of the neutral shock wave profile: propagation at fixed delays (delay time is shown on top of each PAD profile) in reference to the time (t = 0 ms) at which the plasma is switched off, (b) corresponding changes in the velocity of the shock wave in the afterglow plasma. It can be seen that both the shock profile and the velocity recover back to the neutral gas propagation values.

In order to gain some insight into the primary cause of the observed changes in the shock wave velocity and dispersion width, we now analytically investigate various characteristic decay times in the afterglow plasma. To estimate the characteristic decay time for the electrons in the afterglow right after plasma switch-off, the ambipolar diffusion of the electrons to the walls is assumed to be the dominant loss mechanism.[13] In this estimation the characteristic decay time for the electrons is given by $\tau_e = \frac{e}{\mu_i kT_e}\left(\frac{a}{2.4}\right)^2$, where kT_e is the electron temperature in eV, μ_i is the mobility of the ions, and the glow discharge tube radius a = 1.75 cm.[8] The definition of the reduced ion mobility μ_{oi} is given in Ref. 14, and for argon ions (Ar^+) $\mu_{oi} = \mu_i\left(\frac{p}{760}\right)\left(\frac{273}{T_g}\right) = 1.67\ \mathrm{cm^2V^{-1}s^{-1}}$ is obtained from Ref. 15, where p is the pressure in Torr and T_g is the discharge gas temperature in K (assuming $T_i \approx T_g$). At fixed operating pressure p = 15 Torr and calculated discharge gas temperature T_g = 349.6 K, the mobility of the argon ions is estimated to be $\mu_i = 108.35\ \mathrm{cm^2V^{-1}s^{-1}}$. Using this value of the mobility along with the measured electron temperature of $kT_e \sim 1$ eV, the characteristic decay time for the electrons is estimated to be about 4.9 ms. We now estimate the characteristic time τ_T for the centerline temperature to decay to the wall temperature (T_o = 300 K), which is given by $\tau_T = \frac{\rho c_p}{\lambda}\left(\frac{a}{2.8}\right)^2$, where ρ is the gas density, c_p is specific heat at constant pressure, and λ is the thermal conductivity.[16] At fixed operating pressure p = 15 Torr and calculated discharge gas temperature T_g = 349.6 K, the gas density ρ is calculated to be 0.0275 kg/m^3 using the ideal gas law $p = R_A \rho T$, where the gas constant R_A = 208.1 J/(kg.K) for argon. Therefore, the characteristic time for the centerline temperature to decay is about τ_T = 31.6 ms in the argon afterglow plasma using the thermal conductivity λ = 0.0177 W/(m.K), specific heat at constant pressure c_p = 520.3 J/kg.K, and radius a = 0.0175 m.

It is clear from the above calculation of the decay times of 4.9 ms and 31.6 ms for the characteristic electron density and the centerline gas temperature, respectively that the primary cause of the observed changes in the shock wave velocity and dispersion width in the afterglow plasma is the thermal effect since both changes in the shock wave velocity and dispersion take place in the time scale on the order of the characteristic centerline gas temperature decay time of 31.6 ms as shown in Figs. 8(b). During the plasma switch-on, the energy-gain by an electron from the applied electric field and the associated avalanche effect that follows aid in the *breakdown* of the neutral gas, which is known as the Townsend breakdown. The retardation time of the Townsend breakdown is of the order of 0.01–1.0 ms.[13] Thus, a dc glow discharge plasma would be established within the fraction of a millisecond but the heating of the background gas would not take place until after 10's of ms, which is consistent with the measured shock wave velocity and dispersion width as shown in Figs. 7(b). Both changes in the shock wave velocity and dispersion take place in the time scale comparable to the characteristic time for heating of the background gas.

D. Summary of Key Results

- In the steady-state dc glow discharge plasma, at fixed gas pressure the shock wave velocity increases, its amplitude decreases, and the shock wave disperses non-linearly as a function of the plasma current.
- In the pulsed discharge plasma, at fixed gas pressure the shock wave dispersion width and velocity increase as a function of the delay between the switch-on of the plasma and shock-launch.

- In the afterglow plasma, at fixed gas pressure the shock wave dispersion width and velocity decrease as a function of the delay between the plasma switch-off and shock-launch. These changes are found to be opposite and reversing towards the room temperature value which is the initial condition for plasma ignition case.
- Computations yield a characteristic decay time of 31.6 ms for the centerline gas temperature in the afterglow plasma, which closely matches the decay of the shock wave velocity and dispersion width, indicating that the discharge gas temperature is the primary cause of the observed changes in the shock wave velocity and dispersion width.
- During the plasma ignition, the plasma breakdown time has been of the order of 0.01–1.0 ms, thus, a dc glow discharge is established in the tube within a fraction of ms but the heating of the background gas would not take place until after 10's of ms, which is consistent with the measured changes in the shock wave velocity and dispersion width.

IV. On-Going and Future Measurements

The PI's group has just acquired a ¼-m monochromator to study line emissions at the shock-front, and completed some preliminary measurements using narrow band optical filters centered on 515.8 nm line of Ar I. The sketch of the setup and the preliminary emissions from the shock-front is shown in Fig. 9. Additional measurements using this instrument are in progress to investigate the molecular transition lines of nitrogen and atomic lines of Argon. The enhancement in plasma induced emission intensity of the molecular nitrogen C–B line ($C\,^3\Pi_u - B\,^3\Pi_g$) at 337.1 nm and B–A line ($B\,^3\Pi_g - A\,^3\Sigma_u^+$) at 775.4 nm will be measured at the respective wavelength. In parallel, the quenching effect of the Ar I line intensities at the onset of the shock wave propagation in plasma will also be studied. These measurements will be performed as a function of glow discharge reduced electric field E/n at a constant Mach number, and as a function of the Mach number at the constant E/n. The Mach number of the shock wave is varied by charging the capacitor at a different voltage, and the E/n of the discharge can be varied by changing the gas pressure at a constant current.

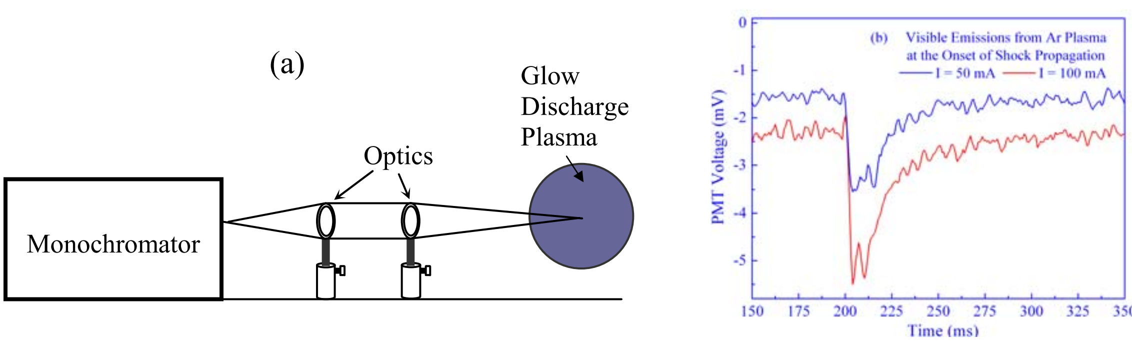

Fig 9: (a) Setup for spectral emission measurements, (b) preliminary total emissions from shock-front at fixed pressure of argon P = 5 Torr and discharge currents I = 50 mA and 100 mA.

The PI has just got funding from the NSF for acquisition of a state of the art spectroscopy instrument. This high resolution monochromator system with fast gated ICCD camera will make possible the investigation of the effects of a weak shock wave (Mach 1–5) on non-thermal plasmas, as well as the interaction of a strong shock wave (Mach 20 or higher) with the plasma in time-resolved spectroscopy in a scale on the order of a ns, and spectral resolution of ~ 0.005

nm. This research will provide new insight into fundamental plasma processes involved in the electronic layers formed at the shock-front. This study will help determine whether the observed enhanced plasma emissions and the associated jump in electron number density can be described entirely by the Mach number or it's dependence on E/n.

V. Student Training and Dissemination of Results

The PI has maintained a very strong commitment to undergraduate student training. The entire Plasma Physics Laboratory was built with the help of undergraduate students. Over the last four years the PI has involved half a dozen undergraduate students in active research, along with few other students in independent and sponsored research projects. Some of these students have already graduated and went on to pursue graduate studies. Presently, the PI has two undergraduate students working with him in various on-going research projects.

When a student comes to work with the PI, he/she participates in a whole range of research tasks from construction and assembly work to daily maintenance and operation of the experiments. Each student is involved in putting together a probe/sensor or using an existing diagnostic to make their measurements. After performing a complete set of measurements, he/she learns to analyze the data using various computer programs. They also carry out a thorough literature search to learn about existing work in the field, and to gather references. The students learn about the relevant theories, examine measurement accuracies, and apply theories to measurements to deduce various parameters. Next, he/she gets training in preparing power point presentation and writing publishable peer reviewed papers on their research results.

Overall, the PI and his team of undergraduate students have been quite active in disseminating the results of these investigations. The PI and his students have already published a total of four papers[9,10,17,18] – three refereed papers in the *IEEE Transactions on Plasma Science*, *Physical Review E,* and *Journal of Applied Physics* and one in the *IEEE Conference Proceedings*. In addition, PI's group has three more papers have currently been either submitted or being reviewed for publication.[11,12,19] Since the funding of the DOE grant in 2004, a total of eight national-level conference presentations[20-27] – five at the American Physical Society's Division of Plasma Physics (APS-DPP), three at the American Physical Society's Gaseous Electronics Conference (APS-GEC), and one at the IEEE International Pulsed Power and Plasma Science Conference, and eight state-level conference presentations at the Alabama Academy of Science (AAS) meeting have been made.

VI. Outreach and Collaborative Activities

In the first two years of the project, the PI coordinated outreach efforts with the lead science teacher Mrs. Shirley Hartin at the nearby Luverne High School, Luverne, AL. In this program the PI ran biweekly physics demonstration classes for the senior students in her advanced physics courses. The PI has been collaborating with Dr. Eugene Omasta and participating in the Alabama *Science-in-Motion* demo classes for the local high schools, and training workshops for the local high school science teachers. The PI's group participated in laboratory tours for the Alabama Academy of Science Conference participants at Troy University in 2006.

The PI has been successful in establishing productive research collaborations with Auburn University, Auburn, AL and Florida A&M University, Tallahassee, FL. He has also started joint measurements with Mr. Lane Roquemore of Princeton Plasma Physics Laboratory (PPPL) in high speed photography of propagating shock wave in plasmas, and with Dr. Peter Bletzinger of Air Force Research Laboratory (AFRL) in shock-front properties in neutral and ionized gasses. These collaborative efforts have already resulted in several conference presentations and peer reviewed publications.

References

[1]P. Bletzinger, B. N. Ganguly, and A. Garscadden, *Electric field and plasma emission responses in a low pressure positive column discharge exposed to a low Mach number shock wave*, Phys. Plasmas **7**, 4341 (2000).

[2]P. Bletzinger, B. N. Ganguly, and A. Garscadden, *Strong double-layer formation by shock waves in nonequilibrium plasmas*, Phys. Rev. E **67**, 047401 (2003).

[3]P. Bletzinger, B. N. Ganguly, and A. Garscadden, *Influence of dielectric barrier discharges on low Mach number shock waves at low to medium pressures*," J. Appl. Phys. **97**, 113303 (2005).

[4]Y. Z. Ionikh, N. V. Chernysheva, A. V. Meshchanov, A. P. Yalin, and R. B. Miles, *Direct evidence for thermal mechanism of plasma influence on shock wave propagation*, Phys. Lett. A **259**, 387 (1999).

[5]S. O. Macheret, Y. Z. Ionikh, N. V. Chernysheva, A. P. Yalin, L. Martinelli, and R. B. Miles, *Shock wave propagation and dispersion in glow discharge plasmas*, Phys. Fluids **13**, 2693 (2001).

[6]S. M. Aithal and V. V. Subramaniam, *On the characteristics of a spark generated shock wave*, Phys. Fluids **12**, 924 (2000).

[7]A. R. White and V. V. Subramaniam, *Shock propagation through a low-pressure glow discharge in argon*, J. Thermo. Heat Transfer **15**, 491 (2001).

[8]N. S. Siefert, *Shock velocity in weakly ionized nitrogen, air and argon*, Phys. Fluids **19**, 036102 (2007).

[9]N. K. Podder, A. V. Tarasova*, and R. B. Wilson IV*, *Shock wave acceleration and attenuation in glow discharge argon plasma*, IEEE Transactions on Plasma Science **35**, 1034 (2007).

[10]N. K. Podder, R. B. Wilson IV *, and P. Bletzinger, *Shock wave propagation in neutral and ionized gases,* Journal of Applied Physics, **104**, 053301-1 (2008).

[11]A. C. LoCascio*, N. K. Podder, A. V. Tarasova*, and A. L. Roquemore, *High speed photography for shock wave propagation in plasma*, being reviewed for publication at the Review of Scientific Instruments (2008).

[12]N. K. Podder and A. C. LoCascio*, *Shock wave interaction with pulsed glow discharge and afterglow plasmas*, Physics Letters A **373**, 1148 (2009).

[13]Y. P. Raizer, *Gas Discharge Physics* (Springer-Verlag, Berlin, 1991), p. 28, 132, & 200.

[14]J. T. Moseley, R. M. Snuggs, D. W. Martin, and E. W. McDaniel, *Mobilities, diffusion coefficients, and reaction rates of mass-identified nitrogen ions in nitrogen*, Phys. Rev. **178**, 240 (1969).

[15]M. Sugawara, T. Okada, and Y. Kobayashi, *Decay processes of atomic ions in low-pressure argon* afterglows, J. Phys. D: Appl. Phys. **19**, 1213 (1986).

[16]N. S. Siefert, B. N. Ganguly, B. L. Sands, and G. A. Hebner, *Decay of the electron number density in the nitrogen afterglow using a hairpin resonator probe*, J. Appl. Phys. **100**, 043303 (2006)

[17]R. B. Wilson IV* and N. K. Podder, *Observation of period multiplication and instability in a*

dc glow discharge, Physical Review E **76**, 046405-1 (2007).
[18]A. V. Tarasova* and N. K. Podder, *Probe diagnostics of high-pressure microwave plasmas for shock wave propagation study*, Proceedings of PPPS-2007, Paper 1812 (2007).
[19]A. V. Tarasova*, N. K. Podder, and E. J. Clothiaux, *Measurements of plasma potential in high pressure microwave plasmas*, under review at the Review of Scientific Instruments (2008).
[20]A. L. Roquemore, N. K. Podder, and A. C. LoCascio*, *Fast photography of acoustic shock waves in glow discharge plasmas*, B. Am. Phys. Soc. **53**(14), 252 (2008).
[21]A. C. LoCascio*, N. K. Podder, and A. L. Roquemore, *Characteristics of a propagating shock wave in gas discharges*, B. Am. Phys. Soc. **53**(10), 18 (2008).
[22]N. K. Podder and A. Locascio*, *Temperature effects on propagating shock waves in glow discharge plasmas*, B. Am. Phys. Soc. **53**(10), 18 (2008).
[23]N. K. Podder, A. V. Tarasova*, and R. B. Wilson IV*, *Shock wave drag coefficients in glow discharge argon plasmas*, Bull. Am. Phys. Soc. **52**(9), 11 (2007).
[24]A. V. Tarasova* and N. K. Podder, *Development and diagnostic of a localized microwave/RF plasma for shock wave propagation study*, 2007 IEEE Pulsed Power and Plasma Science Conference, Albuquerque, MN, June 2007.
[25]N. K. Podder, A. V. Tarasova*, and R. B. Wilson IV*, *Shock wave propagation measurements in glow discharge plasmas*, B. Am. Phys. Soc. **51**(9), 25 (2006).
[26]N. K. Podder, A. V. Tarasova*, and R. B. Wilson IV*, *Shock wave acceleration in weakly ionized plasmas*, B. Am. Phys. Soc. **50**(8), 257 (2005).
[27]R. B. Wilson IV*, N. K. Podder, and A. V. Tarasova*, *Ionization wave chaos in a glow discharge plasma*, B. Am. Phys. Soc. **50**(8), 230 (2005).